Displacement of colloidal dispersions in Porous Media: experimental & numerical approaches

A. Ahmadi-Sénichault[a], V. Canseco[b], N. Sefrioui-Chaibainou[c], A. Omari[d], H. Bertin[e]

I2M, UMR CNRS 5295, Arts et Métiers ParisTech, Bordeaux INP,Université de Bordeaux, France

[a]azita.ahmadi@ensam.eu, [b]vladimir.canseco@ensam.eu, [c]nisrine.sefrioui@ensam.eu, [d]abdelaziz.Omari@enscbp.fr, [e]henri.bertin@u-bordeaux.fr

Abstract The main objective of this paper is to give more insight on colloids deposition and re-entrainment in presence of a rough surface. Experiments on retention and release of colloids in a porous medium are first presented. The influence of physicochemical and hydrodynamic conditions is investigated. The experimental results cannot be qualitatively interpreted using the DLVO theory and knowledges at pore scale are then needed. A 3D numerical simulation approach at the pore scale is therefore proposed where the motion of colloids is solved in presence of collector surfaces bearing various kinds of asperities and by taking into account physico-chemical interactions calculated at each time step during colloid movement. It is obviously observed that both deposition and mobilization of particles are dependent on solution chemistry and hydrodynamic conditions and are significantly affected by the form and size of the local roughness of the pore surface. Therefore, depending on solution ionic strength and surface topography, colloids may be adsorbed or not and when a particle is retained an increase of flow strength is then needed to remove it and such an increase is specific to the location of occurrence of the adsorption step. In general, simulation results allow us to explain our experimental results that show that by steeply increasing the flow strength, more and more fractions of particles retained inside the porous medium are released until all particles are removed.

Introduction

Colloids are small particles whose characteristic size ranges typically from a few nanometers to one to ten micrometers and could be soft or rigid, organic or living micro-organisms and are usually suspended in a background solution of a given composition. In many industrial applications, such dispersions may undergo a flow process in a given geometrical configuration as rectangular channels, impinging jets, or porous media. The flow of colloidal dispersions in porous media are relevant for processes such as filtration, subterranean dissemination of pollutants and wastes, groundwater contamination and water injectivity in oil recovery applications [1]. In a general way, transported colloids in a porous medium may undergo deposition onto pore surface by formation of a mono or even a multilayer deposit.

They can also lead to in-depth formation of bridges and clogging phenomenon as well as straining when their characteristic size is comparable to the size of the pore throats. All these phenomena are gathered under the generic designation of retention and can dramatically modify porous medium properties namely its permeability [2]. Basic laboratory experiments consist in flushing a porous medium column with a well characterized suspension and to follow the characteristics of the out coming fluid. The observed behavior may then be analytically described by a macroscopic continuity differential equation that contains an adsorption source term and can lead to the determination of the adsorption rate [3]. However, when the hydrodynamic conditions and/or the system chemistry is changed, adsorbed colloidal particles may be removed from the pore surface and transported by the bulk flow before they are possibly re-adsorbed elsewhere [4]. Such a process is sometimes called re-entrainment or resuspension and is closely linked to the path that a particle has followed to be adsorbed.

Basically, the porous medium is usually seen as immobile solid grains that act as collectors of the inflowing colloids so a capture efficiency coefficient is defined [5]. This coefficient corresponds to the probability of a colloidal particle to stick onto the collector surface. Such a coefficient is dependent on both the suspending fluid flow and the physico-chemical interactions between dispersed particles and particle/collector and has been extensively considered in the past [6] [7].

Concerning the physico-chemical interaction between particles and between particles and the collector surface, an interaction potential or a disjoining pressure is calculated that includes: the attractive Van der Waals forces and electrostatic forces which, if their additivity is assumed, give rise to the well know DLVO forces [8]. In some cases, the DLVO theory is modified to include short range interactions (Born interaction), then it is usually named extended DLVO theory. Steric interactions are also included if particle and/or collector surface are coated with polymers [9]. The disjoining pressure may be easily calculated as a function of the separation distance, knowing particle and collector sizes, the relative permittivities and the zeta potentials of the involved materials and the ionic strength and pH of the suspension. It generally consists in an energy barrier that is surrounded by a primary minimum and a secondary minimum, which for given particles and porous medium will practically depend on the pH and the salinity of the background solution. At low separation distances, DLVO interaction potential (or the disjoining pressure) may become greater than drag forces and is determinant in adsorption/desorption mechanisms. Therefore when the height of the energy barrier is very low, every particle that comes into contact with the collector is retained and the adsorption process is called favorable. On the contrary, for significant heights of the energy barrier, the adsorption is called non-favorable.

It is obvious that for adsorption/desorption processes both hydrodynamic and physico-chemical interactions are important and particles do concomitantly experience both force types. However adsorption and mobilization are usually considered by studying separately the flow impact and the influence of particle/particle and particle/collector physico-chemical interactions. Therefore, keeping the flow rate constant, the adsorption-desorption processes are investigated by modifying the DLVO potential through changes in pH, salinity or both.

Some experimental evidences show that even if the DLVO theory allows qualitative predictions; it falls quantitatively. Discrepancies were alternatively attributed to chemical heterogeneity of surfaces and surface roughness [7][8][10] inducing a change in magnitude and location of minima and the barrier. In a previous work we have investigated such a process for a large range of ionic strengths [11] and showed that colloidal particles do adsorb preferentially in (and desorb from) the secondary minimum as suggested by several authors [7] [12] [13].

If the physico-chemical potential is kept constant, previous experimental works have shown that by increasing the flow strength a fraction of already adsorbed particles may be desorbed due to flow. Several mechanisms are usually put forward to describe mobilization of adsorbed particles: by rolling when the torque is greater than the torque of adhesion forces; by sliding when the drag force overcomes the particle/surface frictional force or by lifting when the lift force is greater than the adhesion force [14]. Bergendhal et al. [15] have estimated the drag force that is needed to mobilize a deformable particle that is adsorbed in close contact with a significant surface asperity underlying hence the role of surface roughness in mobilization process. Sharma et al. [16] have reported that the fraction of re-suspended particles does increase when surface roughness increases within the submicron range while it is seemingly lower for surface roughness in the micro-scale. In fact, the rate of re-suspension depends on the details of surface topography, namely the characteristic height and the density of surface asperities and such roughness does play a complex role in particle adsorption and their possible re-entrainment as it impacts both the interaction potential as well as the flow structure in the vicinity of the wall surface [17].

In this paper we are mainly concerned by the re-entrainment process subsequent to a well characterized adsorption step. As particles re-entrainment is dependent on the adsorption mechanisms, therefore adsorption is addressed beforehand. Moreover, while experiments are performed on centimetric cores, direct numerical simulations are performed at the microscale in order to clarify some of the explanations put forth to describe the retention/release behavior. In the next part the characteristics of used materials and the experimental set up are given, the followed procedure is described and the experimental results are presented and discussed. The second part is devoted to present the in silico-experiments by emphasizing how numerical simulations are run and simulation results are presented and discussed. The paper ends with some conclusions and the forthcoming investigations.

1) **Experiments**

The objective of this part is to perform retention/release experiments in a consolidated porous medium using calibrated colloidal particles. Some results dealing with the influence of ionic strength have already been published [11] and a focus will be laid here on the effect of hydrodynamics on the particle release but as mobilization of particles depend on deposition step, we will also briefly present some characteristics of such a deposition step.

1.1) Materials and methods.

- *Porous medium*

In this work, an artificial consolidated core, Aerolith-10® (from Pall Corporation) made from sintered silicate grains was used. The porous media are available in the form of cylinders with a circular cross section (D = 5 cm). This core, commonly used for filtration purposes, known to be relatively homogeneous and water wet has a porosity of 43% and a permeability of around 8.10^{-12} m^2. More specific details can be found in (www.Pall.com). The porous media samples whose length may vary from 5 to 15 cm are epoxy coated and inlet and outlet devices with valves are mounted to insure fluid injection and pressure drop measurements. The zeta potential of the silicate grains have been measured [11] showing negative values for all our experimental conditions.

- *Colloidal particles*

Surfactant free polystyrene latex micro-spheres (IDC, Portland, OR) with a mean diameter equal to 780 nm and a negative zeta potential under our experimental conditions was used. It is worth noting that the zeta potential of the colloidal particles is always lower than the zeta potential of the collector grains [11]. The colloidal particles are diluted in the background solution at a concentration (C_0) of 200 ppm.

- *Solution chemistry*

The background solution was prepared with deionized water and potassium iodide (KI). This salt was used as a contrast agent for improving γ-rays attenuation measurements. The pH was adjusted to 7.0 and sodium azide (NaN_3) was added as a bactericide.

1.2) Experimental setup and procedure

The experimental setup is presented in Figure 1
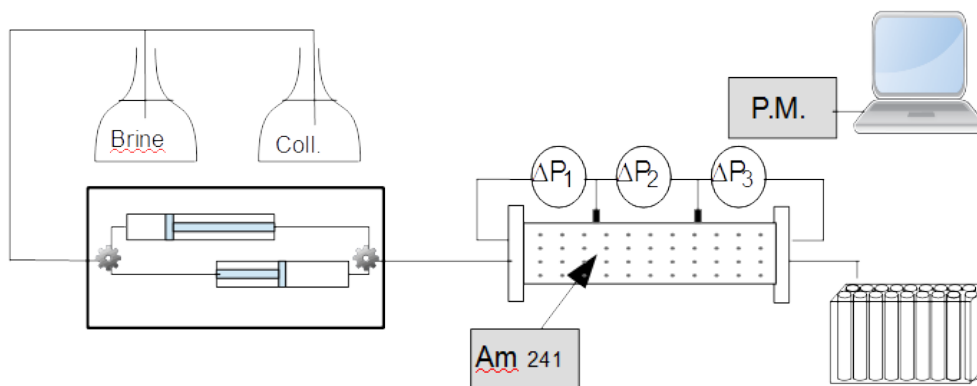
Figure 1 - Experimental setup.

The fluids, brine or colloidal suspension, are injected in the porous medium using a volumetric pump with a flow-rate variable from 1 to 499 ml/h. The pressure drops are

measures along the core using three differential pressure transducers (Rosemount). Effluents are collected and colloidal concentration is measured using a spectrophotometer. The porous medium is positioned horizontally in a rig displacing a γ-rays attenuation apparatus for porosity measurement. This apparatus is made up of a radioactive source (Americium 241) and a crystal scintillator (NaI) associated with a photomultiplier (PM). The principle of γ -rays attenuation technique applied to colloid deposition in porous media is based on the selective attenuation of γ -rays by solids and fluids which is described in details in another work [18]. Note that the counting time necessary to measure a local porosity value is of 30 minutes which implies that colloidal suspension injection should be stopped during porosity field measurement.

The experimental procedure starts with the γ-rays counting on the dry medium before background solution saturation. The initial local porosity is then measured. Colloidal suspension injection is then started in a discontinuous way (Experiment I) or continuous one (Experiment II).

Experiment I

Colloidal suspension is injected at a constant flow rate, corresponding to a Péclet number of Pe = 9.8 (defined by Eq. 1), for time values corresponding respectively to 3.5 PV, 5.5 PV, 6.5 PV, 10 PV, 15 PV and 25 PV. The unit PV corresponds to the time necessary to inject one pore-volume in the porous sample.

$$Pe = \frac{U d_p}{D} \tag{1}$$

Where U is the local velocity or the Darcy velocity, d_p the particle diameter and D the diffusion coefficient.

Between each colloidal suspension injection, the background solution (I = 7.2 mM) is injected to displace the mobile particles from the core and local porosity field is measured by γ -rays. The complete sequence is repeated 7 times for a total volume of colloidal suspension injection equal to 25 pore volumes (PV).

Experiment II

The first step of this experiment corresponds to a particle adsorption performed at a Péclet number of 9.8 during colloidal suspension (I = of 7.2 mM) injection of 20 pore volumes. This adsorption step is followed by a background solution injection of 3 pore volumes to displace the mobile particles from the core. When such displacement was completed, pure water (I = 0M) is then injected at a Péclet number of 15 until the particle concentration in the effluents goes back to zero. The flow rate is then increased and particle concentration in the effluents is measured until it falls to zero before increasing again the flow rate and so on. In our experiments the scanned Péclet numbers range from 15 to 50.
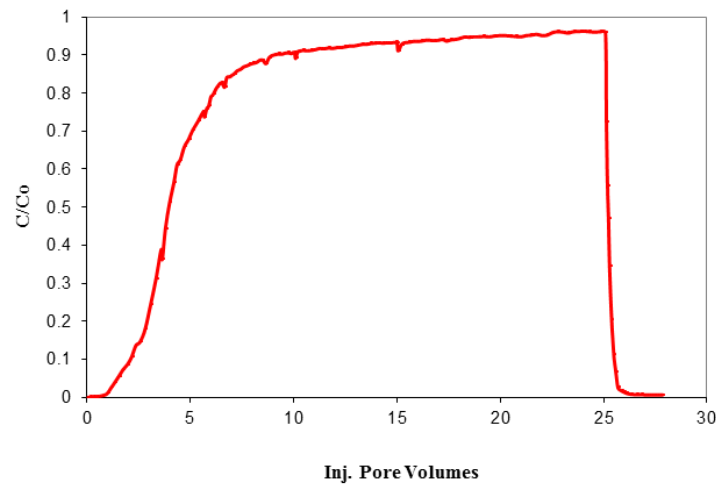
1.2)   Results and discussion.

- *Experiment I*

The step by step adsorption is presented in Figure 2 while the cumulative adsorption curve, taking into consideration only the deposition steps (without the flushing ones) is presented in Figure 3.
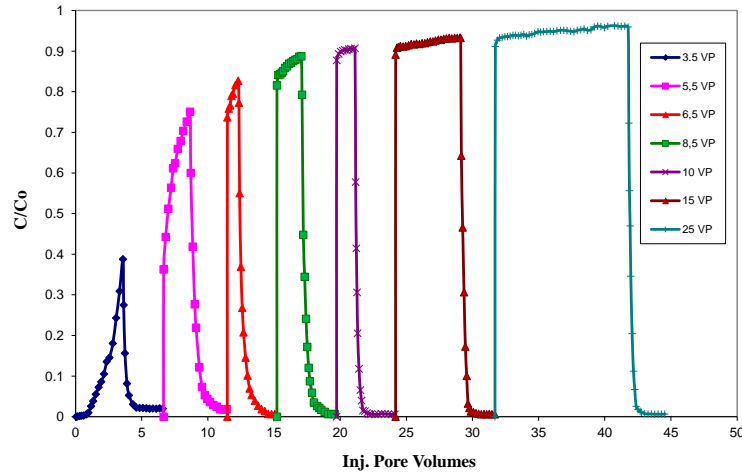

Figure 2 - Colloidal suspension injection and flushing steps.

Figure 3-: Breakthrough curve corresponding to the adsorption steps.

The shape of the breakthrough curve is as expected showing a quick increase of the particle concentration at the first stages of the experiment and a stable value, close to 1, at the end of the experiment corresponding to the end of the deposition process. At that ionic strength and hypothesizing smooth surfaces, the disjoining pressure calculated by means of the extended DLVO theory shows a primary minimum Φ_{min1}= -56 kT, a barrier height Φ_{max}=73 kT and a

secondary minimum of depth $\Phi_{min2} = - 0.5$ kT, where kT is the Boltzmann's factor (see Figure 4).
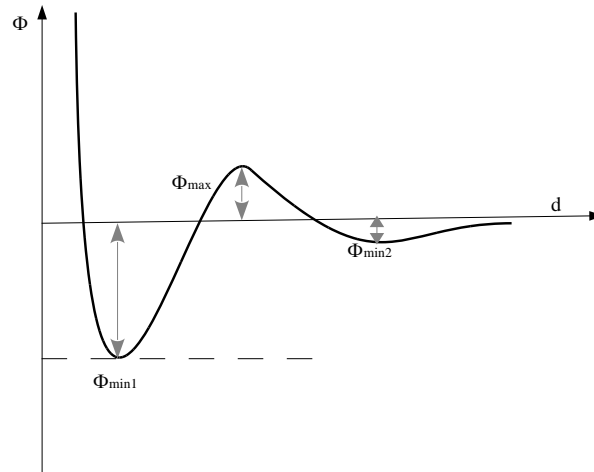
Figure 4 - Particle-collector disjoining pressure as a function of collector particle separation distance d.

This shows that for the particles to be adsorbed in the primary minimum, they have to overcome a high energy barrier so that they should be preferentially adsorbed in the secondary minimum. In other words and for a given flow rate, the adsorption constant in the primary minimum is much less than in the secondary minimum and both are dependent on pore surface coverage which depends on hydrodynamic conditions. [19] [20]. This gives a qualitative description of the behavior observed in Figure 3. Such a breakthrough curve is usually well fitted by the analytic solution of a dispersion equation that includes an adsorption source term in case of semi-infinite porous media and hence leads to the value of the adsorption constant. In Figure 5 the porosity fields of the core measured along the axis after the different stages of the deposition process are plotted.
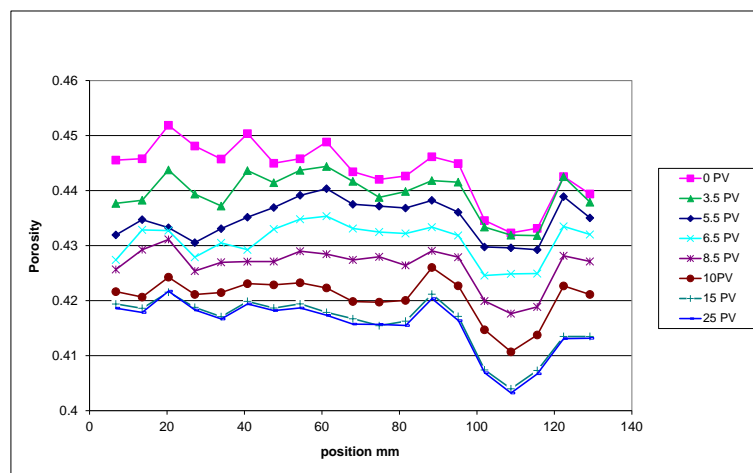
Figure 5 - Porosity fields along the core after the adsorption steps of Figure 2.

First of all it can be noted that the porous medium is not really homogeneous as its initial porosity values vary from 0.451 to 0.431. It is clearly seen that porosity decreases gradually as the colloidal suspension is injected. If the porosity field measured after 3.5 PV injected is considered, it is clear that the porosity reduction, corresponding to a decrease of the pore volume due to particle deposition, occurs mainly in the core entrance while it is not modified at the core exit. When colloidal suspension injection is resumed, a constant porosity decrease all along the core is observed until 15 pore volumes are injected. Beyond this value there is almost no porosity change along the core. This behavior indicates that the deposition process is gradual and occurs like a dispersed front traveling along the core with a transfer of moving free particles in the suspension towards the solid phase. The constant final value of adsorbed particles (Figure 3) and the stabilization of the porosity field is clearly the evidence that deposition occurs as a monolayer on the solid surface as it would be expected since the particle-particle interaction is repulsive in our conditions.

The hydrodynamic thickness δ of the deposited layer can be estimated by assuming that the porous medium is well represented by a bundle of capillary tubes of the same radius as [21]:

$$\delta = R_p(1 - R_k^{-1/4}) \tag{2}$$

where R_p is capillary tube radius calculated from

$$R_p = \sqrt{8k / \phi} \tag{3}$$

where k is the permeability and ϕ is the porosity of the sample and

$$R_k = \frac{k_i}{k_d} = \frac{\Delta P_i}{\Delta P_d} \tag{4}$$

is the permeability reduction where the subscripts i and d indicate initial and damaged value after colloidal deposition that are determined through measurement of pressure drop on the initial and damaged porous medium, ΔP_i and ΔP_d respectively.

The results presented in Figure 6 confirm that deposition is a continuous process along the core starting at the entrance and that the final value of the layer thickness is constant along the core and equal to 0.7µm, value which is close to the colloid diameter (0.78 µm) confirming the monolayer deposition. It is worth noting that, for a single deposited sphere, the equivalent hydrodynamic thickness is theoretically predicted to be equal to 0.82 d_p giving $\delta=$ 0.64µm [22].
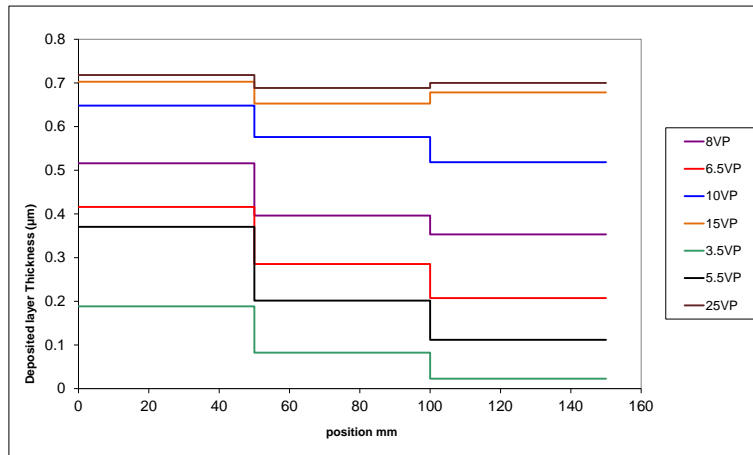
Figure 6 - Hydrodynamic layer thickness along the porous medium at different steps of colloidal suspension injection.

- *Experiment II*

In a previous study we have shown that given ionic strength conditions under which adsorption has been performed (particular depths of minima and height of the energy barrier), flushing the porous medium by water of decreasing ionic strength leads to the mobilization of a fraction of the adsorbed particles. It was also shown that assuming that particles are already adsorbed in the secondary minimum and they behave as a Maxwell gas trapped in a potential well, the removed particle fraction may be predicted at least qualitatively [11].This experiment starts with a colloidal suspension injection (I = 7.2mM, Pe = 9.8) followed by pure water injections (I = 0M) for which the second minimum disappears at different values of Péclet number. The results are presented in Figure 7.
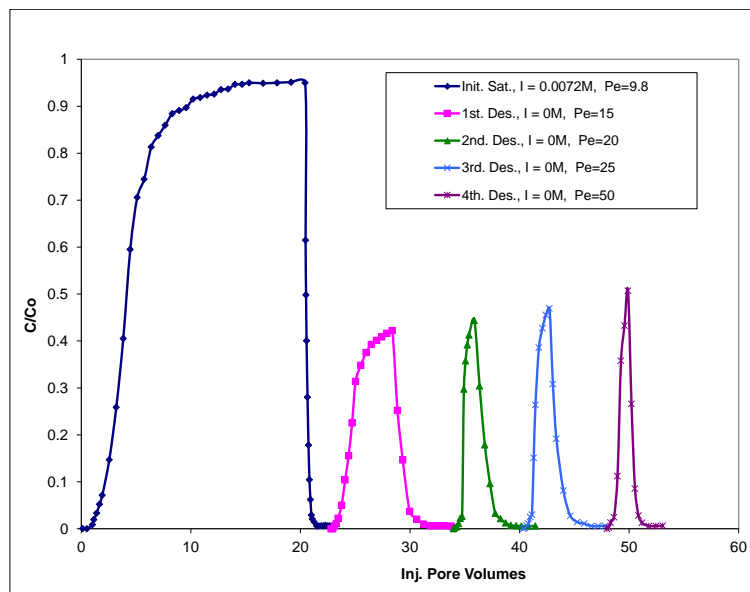
Figure 7 - Adsorption followed by successive desorption steps by increasing the Pe number.

The adsorption step is as expected, the relative concentration of colloidal particles in the effluents is almost stable after the injection of 15 pore volumes and its value is close to 1. When pure water is injected in the core at a Péclet number of 15, a smooth increase of the concentration is clearly observed corresponding to particles desorption. A maximum value of colloidal concentration is obtained after injection of 5.3 pore volumes of water then colloidal concentration decreases quickly to reach a zero value. When Péclet number is increased to 20, a new quick increase of the concentration followed by a concentration decrease is again observed. A similar behavior is noticed when Péclet number is increased to 25 and then to 50. However a behavior difference between the BT curves when the Péclet is increased is remarked. In our previous study [11] it has been shown that if Péclet number is low (Pe=4) the rate of removal process is constant and a large plateau in the BTC is observed. In the present study it is clear that desorption curve is less and less smoother as Péclet number is increased and this can be attributed to the growing influence of convection relative to diffusion as Pe increases and this can be phenomenologically explained as follows: if we assume the adsorbing surface is rough so that the population of adsorbed particles is constituted of particles adsorbed on smooth surfaces plus particles adsorbed in cracks and in vicinity of asperities, only those adsorbed on smoothest surfaces are removed at low Pe numbers. By increasing the Pe, the hydrodynamic forces become high enough to remove the other particle populations trapped in cracks and standing against asperities.

The cumulative mobilized particle fraction is plotted in Figure 8 as a function of Péclet number. We clearly see that the cumulative number of desorbed particles increases with Péclet number. At the end of the experiment almost 95% of the adsorbed particles are released from the core as already observed in the literature in case of flat adsorbing solids [23].
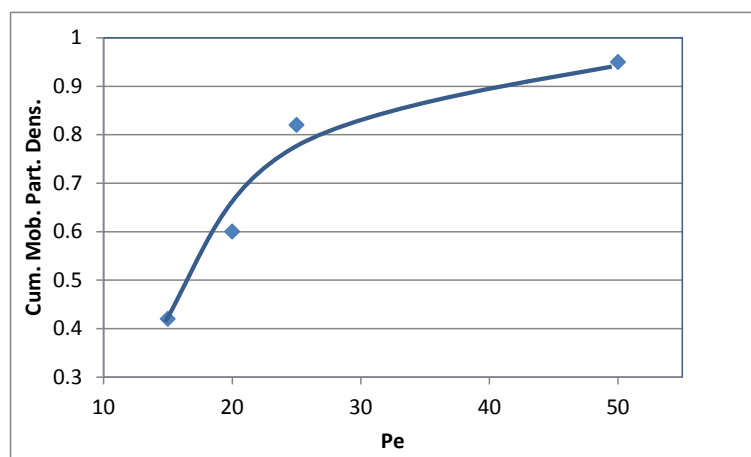
Figure 8 - Cumulative mobilized particle density as a function of Péclet number.

As mentioned before, Particles removal can occurs by rolling, sliding or lifting depending on the forces acting on adsorbed particles. Our results suggest that the pore surface topographic heterogeneity should play an important role in mobilization process. At low Pe diffusion is dominant and particle that are adsorbed on smooth surfaces are easily removed by rolling at a constant rate. For particles that are trapped in surface part involving asperities, higher drag and lifting forces are needed to dislodge such particles. Of course a broad asperities size

distribution is expected to exist (height, form, density, etc.) and only a fraction of them is removed at a given Pe number.

To get more insight in the removal mechanism in case of a pore surface having topographic heterogeneities, a direct numerical simulation may be an efficient tool.

3. Numerical simulations at the microscopic scale

In this section, direct numerical simulations of retention and release of micron sized colloidal particles near a grain surface are performed. The simulations are based on a numerical code developed in our laboratory in which special modules were implemented to take into account hydrodynamic and physicochemical interactions in the vicinity of a pore-surface with roughness of various shapes and characteristic sizes [24]. In the next section, the main features of the model are recalled before presenting some results on the influence of pore-surface roughness, physicochemical interactions and hydrodynamic conditions on the retention and release of particles.

3.1. Configuration

The experimental conditions presented in the previous section are used as a basis for the choice of geometrical and physical parameters used in numerical simulations. Therefore, dispersions of negatively charged colloidal latex particles of radius, $a_p = 400$nm are injected in an artificial sintered silicate of 0.43 porosity and 8×10^{-12} m^2 permeability. The Péclet and particle Reynolds numbers Re$_p$ (Re$_p$= U a_p/ν, ν being the kinematic viscosity of water) is respectively equal to 9.8 and 1.66×10^{-5} in accordance with the values used in laboratory experiments. This leads to a mean velocity at the inlet of 4×10^{-5} m.s^{-1} for the numerical simulations.

The simulations are limited to a small domain of 5 µm x 4µm x 3.8 µm near a pore surface, where the colloid is placed on the symmetry plane of the domain at a fixed position at the initial time. Besides the modification of the hydrodynamics in the vicinity of the pore-surface, roughness impacts the magnitude of physicochemical interaction potential between the particle and the pore-surface. Different asperities are considered as follows: smooth surface (no asperities), right triangular prisms of the form of peaks or valleys of height H equal to a_p or $2a_p$ and - a_p or -$2a_p$ respectively (Fig. 9).

The influence of physicochemical interactions between the particles and the pore-surface on the retention and release is studied through three different magnitudes of DLVO forces. For fixed values of Pe and Re$_p$ and for each roughness, these magnitudes are obtained by calculating the disjoining pressure for three different values of salinity (0.5, 1.2 and 2 or 3 g/L of NaCl) corresponding to three levels of ionic strength, I, designated by weak (I = 3 mM), medium (I = 7.8 mM) and strong (I = 12 or 18 mM). The pH was set constant at pH=7.

3.2. Governing equations

The numerical code Thetis® developed in I2M laboratory is used to perform direct numerical simulations. Within the framework of this work, additional modules have been added in order to take into account particle/particle and particle/grain-surface physicochemical interactions [24]. The transport of particles is modeled using a generalized one-fluid model [25] and a unique set of governing equations, Navier Stokes and masse balance, is therefore considered for the global fluid phase:

$$\nabla.\mathbf{u} = 0 \tag{5}$$

$$\rho\left(\frac{\partial\mathbf{u}}{\partial t} + (\mathbf{u}.\nabla)\mathbf{u}\right) = -\nabla p + \nabla.\left(\mu(\nabla\mathbf{u} + \nabla^t\mathbf{u})\right) + \mathbf{F_s} \tag{6}$$

where $\mathbf{u}$, ρ, p and $\mathbf{F_s}$ are respectively the velocity, the fluid density, the pressure, and a source term corresponding to areal and volumetric volume forces. Since the physical conditions considered in this work allow us to neglect gravity, $\mathbf{F_s}$ only includes particle-grain DLVO and lubrication forces.

The boundary conditions imposed are constant flow rate at the inlet, a Neumann condition on the velocity at the outlet and no-slip boundary conditions on the lateral and bottom surfaces. A slip velocity was imposed at the top surface of the domain.

Within the global fluid, the solid particle is distinguished from the liquid through a phase indicator function, F_c. The displacement of the particle is described through the resolution of a transport equation for F_c.

$$\frac{\partial F_c}{\partial t} + u.\nabla F_c = 0 \tag{7}$$

In this work the computation of DLVO forces between a spherical particle and a rough grain surface is performed by the Surface Element Integration (SEI) method [24] [26] [27] [28] at each step of the particle pathway.

3.3. Numerical model

Fixed Cartesian grids are chosen and the particle diameter contains 16 blocks following other works in the literature [25] [29].

The numerical model used in Thetis® is based on an implicit tensorial penalty method [30]. In this method, a special decomposition of the stress tensor allows to impose incompressibility in the fluid and undeformability for the solid. The reformulated Navier Stokes equations are solved using a finite volume method on staggered grids, where a second order centered scheme is used for approximating the terms. The algorithm used is based on the augmented Lagrangian method which allows coupling the velocity and the pressure while keeping an implicit method. An Eulerian Lagrangian Volume of Fluid method is used for resolution of the transport of the indicator function F_c.

3.4. Results and discussion

- *Retention*

For the five topographical configurations mentioned above and the three ionic strength levels, numerical simulations have been performed. The results in terms of particle trajectory are summarized in Fig. 9 and are calling the following comments.

When the particle is in the vicinity of a smooth surface, it is attracted towards the pore-surface for medium and strong ionic strengths. Indeed, although at the separation distance considered here between the particle and the pore-surface the DLVO forces are attractive but they are weak and hydrodynamic forces still dominate. The particle is therefore attracted to the surface but continues its trajectory out of the computation domain under the influence of the flow. For a weak ionic strength however, the DLVO forces are repulsive and drive the particle away from the pore-surface. Moreover, from the velocity fields, it can be noted that the particle displacement corresponds, as expected, to a combination of rotation and translation (data not presented here).

For peaks 1 and 2 and weak and medium ionic strengths, the particle overpasses the obstacle and comes in contact with the pore-surface without sticking after having over passed the wake of the obstacle. For the strong ionic strength, the particle approaches the wall due to attractive particle-surface DLVO forces and is blocked at the foot of the peak. In this case the particle is retained and will not move any more.

For the valleys and weak and medium ionic strengths, the particle continues its displacement until exiting the domain as for peaks. The dissymmetry observed in the trajectory of the particles is due to the recirculation zones at the bottom of the valleys on the one hand and to the hydrodynamic forces (pulling off) that push the particle in the direction of the bulk flow on the other hand. For valley 1 and the strong ionic strength, although the particle undergoes strong attractive DLVO forces, its displacement is not blocked and it continues its movement while for deeper valley (Valley 2), the particle is retained in the valley.

- *Release*

As observed in the last section, in three configurations and only for the case of a strong ionic strength, the particle is retained on the pore surface: for the two peaks and the deeper valley. The particle retained in these cases, can be released through two different processes: either keeping the same physicochemical conditions (i.e. same salinity), the flow rate is increased or keeping the same hydrodynamic conditions (flow rate) and injecting a brine of lower salinity (lower ionic strength). As a first approach, for the same ionic strength, the Reynolds number has been increased.

It is therefore necessary to choose a particle Reynolds number higher than the one used for retention ($Re_{p1}= 1.6 \times 10^{-5}$). For the case of peak 2 and for $Re_{p1}= 1.6 \times 10^{-5}$, at the retention point, denoted O_P (for strong I), the ratio of the x and y components of the hydrodynamic forces,

F_{Hydro} , over the DLVO forces, F_{DLVO}, are respectively $F_{Hydro,x}/F_{DLVO,x}$=-2 and $F_{Hydro,y}/F_{DLVO,y}$= -1. In order to propose an estimate of a Re_p value which would lead to particle release, the same ratio is calculated around the same position O_P for the case of weak ionic strength as for this case, the particle was not retained and continued its displacement. For an x-position corresponding to that of O_P, the ratios $F_{Hydro,x}/F_{DLVO,x}$ =100 and $F_{Hydro,y}/F_{DLVO,y}$ =-30 were then chosen. This ratio is one to two orders of magnitude higher than the ones obtained for the case of strong ionic strength.

Estimates of the particle Reynolds number leading to approximately the same behavior as that potentially obtained by decreasing the ionic strength leads to the value of Re_{p2}=8.3 10^{-4} and Re_{p3}= 1.66 10^{-3} which are respectively 50 and 100 times higher than the value used for retention.

In order to study particle mobilization at its incipient stages, simulations of flows over short periods of time with Re_{p2} and Re_{p3} have been performed. It is therefore observed that this increase of Re_{ep} leads to the mobilization of the colloidal particle for all three cases where retention was observed previously (Peak 1, Peak 2 and Valley 2). Moreover, while for both Re_{p2} and Re_{p3} the particle trajectories at the onset of mobilization are superimposed, the mobilization velocity varies as a function of Re_p and the roughness. In figure 10, displacement distances are presented as a function of time for the three asperities and the two Re_p considered. From these results it can be noted that:

- All curves have the same tendency, i.e. a quasi-linear variation of the displacement as a function of time pointing out a constant average particle velocity.
- For the two peaks, for both values of particle Reynolds number considered here, the particle travels nearly the same distance over the same period of time.
- For each particle Reynolds number considered, the distance traveled by the particle in presence of Valley 2 is shorter than the one traveled in presence of the peaks. The particle average velocity is therefore smaller for the case Valley 2 than for the two peaks considered. For the cases studied here, the average particle velocities for release are listed in table 1.

	$Re_{p2} = 8.3\ 10^{-4}$	$Re_{p3} = 2\ Re_{p2}$
Peak 2	7.42 10^{-5}	1.56 10^{-4}
Peak 1	7.42 10^{-5}	1.59 10^{-4}
Valley 2	2.97 10^{-5}	4.17 10^{-5}

Table 1 – Average particle velocity after release.
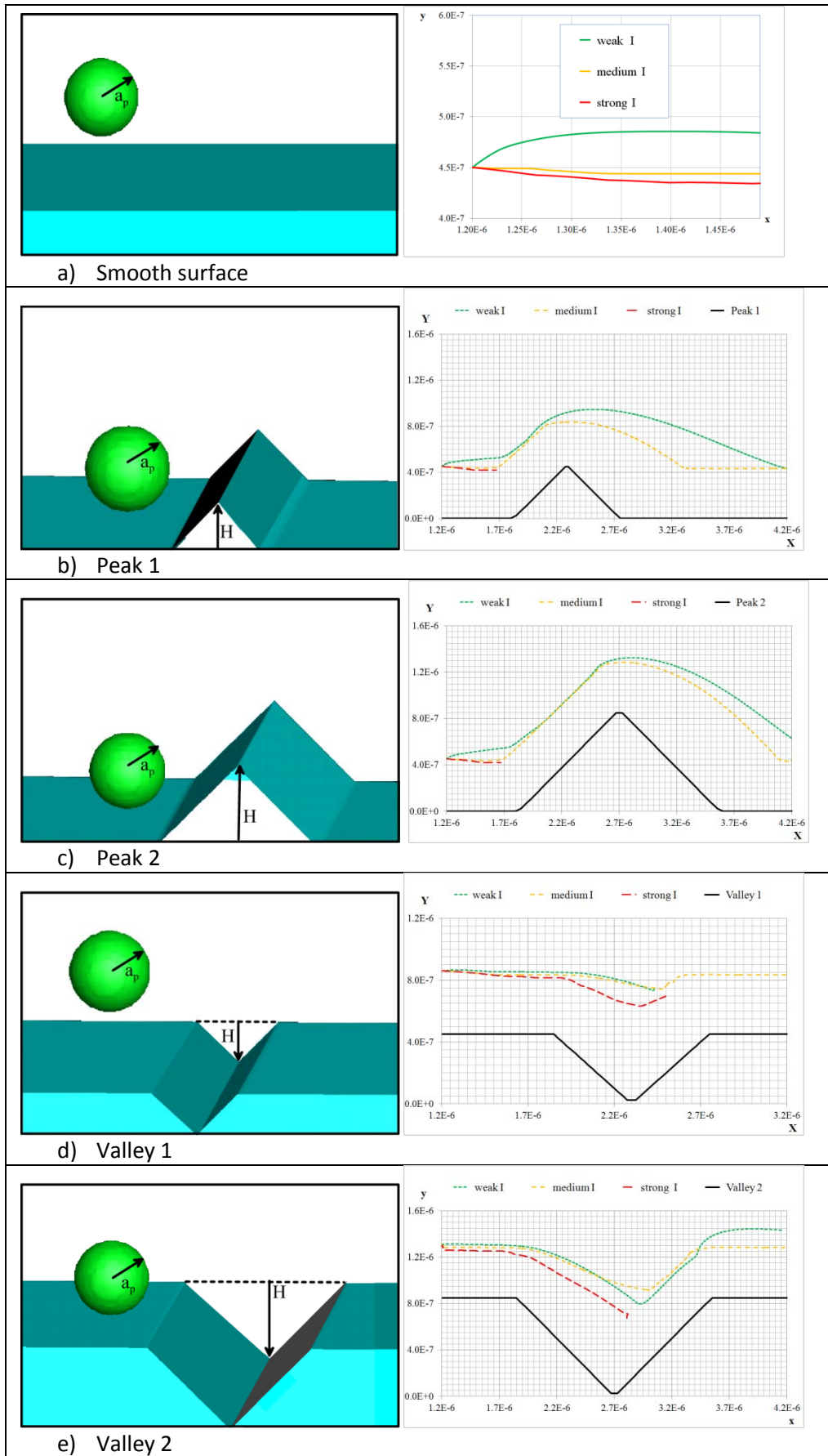
Figure 9 - Representation of the five geometrical configurations considered and the associated trajectories for $Re_{p1} = 1.6 \ 10^{-5}$ and three different ionic strength levels.
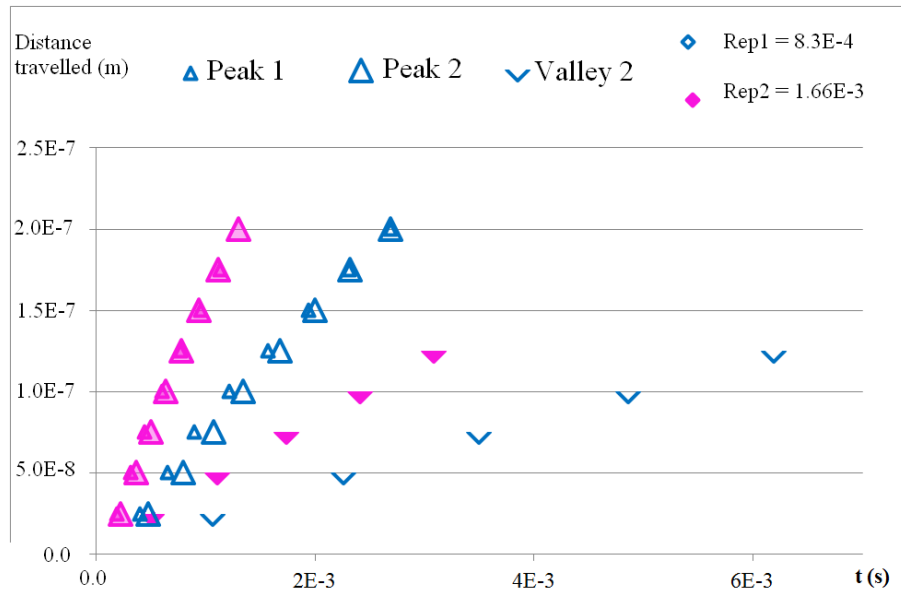
Figure 10 - Distance traveled as a function of time during release of particles in presence of roughness for two different values of Re$_p$.

- *Discussion*

In order to synthesize the influence of roughness and ionic strength for a given Rep, the residence time of the particle in a given domain is considered. The central part of the simulation domain is considered in order to avoid possible perturbations related to inlet and outlet boundary conditions.
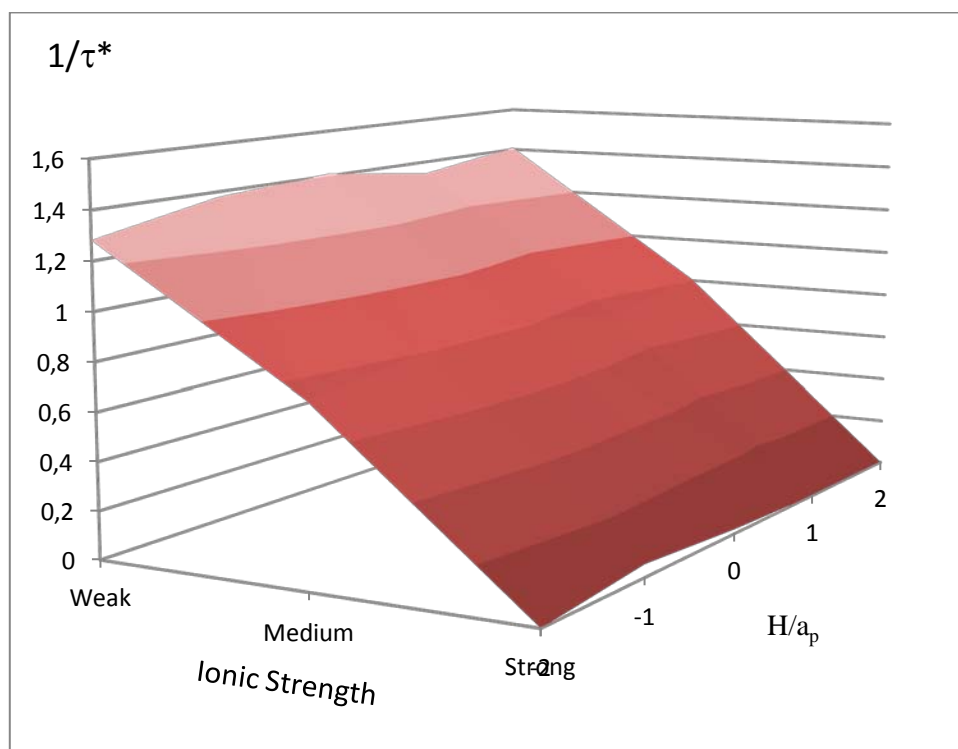
In Fig. 11 the inverse of the dimensionless residence time τ^{*-1} is plotted as a function of the ionic strength and the roughness represented by the ratio H/a$_p$. The reference time used for the calculation of τ^* is the time needed for a particle to travel through the flat surface for a zero ionic strength.

For a given Re$_p$, the dominant factor in the variation of the residence time is the ionic strength (Fig. 11). The residence time decreases as the ionic strength decreases. A close investigation of the residence time for strong ionic strength reveals that τ^{*-1} tends to zero for the three cases where retention was observed previously (peaks 1 and 2 and valley 2). However, although τ^{*-1} seems very small for the case of a smooth surface and valley 1, its value is 4 orders of magnitude larger than the values for the two peaks and the valley 2. This corresponds to a smaller yet finite residence time for these two cases. It can be noted that, whatever the value of the ionic strength, the particle can not be retained near a smooth surface. This may be explained by the fact that the physicochemical interaction forces for rigid materials are central and particles may rotate freely while translating in parallel to solid surface even if they are attracted to grain surface.

Even though they are partial, all these qualitative but rigorous observations can serve as a basis to explain the experimental evidences presented in the previous section which were phenomenologically interpreted. We see therefore that even though the DLVO forces and their monitoring through change of the background solution chemistry play a major role in

retention and release of colloids during flow in porous media, heterogeneity (topography and composition) of the surfaces coming in contact are also important. Such heterogeneities indeed affect the disjoining pressure both in magnitude and range and the presence of surface asperities bring additional modifications of the flow structure in the particle/grain contact region influencing hence both retention and release of particles. This was already experimentally observed by other authors through direct observation [31] [32] [33].

It should be emphasized here that after the adsorption step, when the ionic strength is lowered to zero (suppressing the secondary minimum) at a low Péclet number, only a fraction of already adsorbed particles are recovered [11]. This means that some particles trapped in topographic heterogeneity sites are still retained and sufficient hydrodynamic forces are needed to remove them as seen in Figure 8. It is however obvious that our simulations are partial and give only some trends and they should be continued by screening a large range of Reynolds numbers.

Figure 11 – Inverse of the dimensionless residence time as a function of ionic strength and roughness (H/a_p).

4. Conclusions

In this study we investigated some aspects of retention and release of well characterized colloids in porous media by carrying out experiments and performing numerical simulations in which pore surface roughness was taken into account. Our investigation mainly focused on release phenomenon even some aspects regarding retention are also presented. In the experimental study, it was successively shown that:

- For a given hydrodynamic conditions and suspension chemistry, the colloids deposition process is "piston-like" and the deposited layer at the end of the process is a monolayer. Moreover the equivalent thickness of such a layer is nearly the same when it is deduced from the breakthrough curves or determined using the γ-rays attenuation technique.
- After the deposition step, when the porous medium is flushed by pure water at increasing Péclet number, the cumulative fraction of removed colloids increases until all already deposited particles are recovered.

These experimental results were phenomenologically interpreted by putting forward the role that should play the pore surface roughness in deposition and release processes. To sustain such interpretation, some in silico-experiments were performed at pore scale using 3D direct numerical simulations of deposition and release of isolated particles at various ionic strengths and hydrodynamic conditions in presence of different kinds of roughness. From theses preliminary simulations, it was shown that, depending on the roughness under interest and given the hydrodynamic conditions, the colloids may be attracted to or repealed from the pore wall and they may be retained at some specific locations. It was also shown that when the particle is trapped, increasing the flow strength yields re-suspension of the particle due to a favorable hydrodynamic /physic-chemical force balance. Indeed, these simulations should be continued on a large range of Reynolds number to get more quantitative insight in involved phenomena.

References

[1] J. Moghadasi, H. Müller-Steinhagen, M. Jamialahmadi, and A. Sharif, "Theoretical and experimental study of particle movement and deposition in porous media during water injection," *J. Pet. Sci. Eng.*, vol. 43, no. 3, pp. 163–181, 2004.

[2] C. Henry and J.-P. Minier, "Progress in particle resuspension from rough surfaces by turbulent flows," *Prog. Energy Combust. Sci.*, vol. 45, pp. 1–53, 2014.

[3] A. Zamani and B. Maini, "Flow of dispersed particles through porous media: deep bed filtration," *J. Pet. Sci. Eng.*, vol. 69, no. 1, pp. 71–88, 2009.

[4] W. P. Johnson, X. Li, and S. Assemi, "Deposition and re-entrainment dynamics of microbes and non-biological colloids during non-perturbed transport in porous media in the presence of an energy barrier to deposition," *Adv. Water Resour.*, vol. 30, no. 6, pp. 1432–1454, 2007.

[5] K.-M. Yao, M. T. Habibian, and C. R. O'Melia, "Water and waste water filtration. Concepts and applications," *Environ. Sci. Technol.*, vol. 5, no. 11, pp. 1105–1112, 1971.

[6] J. N. Ryan and M. Elimelech, "Colloid mobilization and transport in groundwater," *Colloids Surf. Physicochem. Eng. Asp.*, vol. 107, pp. 1–56, 1996.

[7] N. Tufenkji and M. Elimelech, "Breakdown of colloid filtration theory: Role of the secondary energy minimum and surface charge heterogeneities," *Langmuir*, vol. 21, no. 3, pp. 841–852, 2005.

[8] Z. Adamczyk and P. Weroński, "Application of the DLVO theory for particle deposition problems," *Adv. Colloid Interface Sci.*, vol. 83, no. 1, pp. 137–226, 1999.

[9] D. Grasso, K. Subramaniam, M. Butkus, K. Strevett, and J. Bergendahl, "A review of non-DLVO interactions in environmental colloidal systems," *Rev. Environ. Sci. Biotechnol.*, vol. 1, no. 1, pp. 17–38, 2002.

[10] S. Bhattacharjee, C.-H. Ko, and M. Elimelech, "DLVO interaction between rough surfaces," *Langmuir*, vol. 14, no. 12, pp. 3365–3375, 1998.

[11] V. Canseco, A. Djehiche, H. Bertin, and A. Omari, "Deposition and re-entrainment of model colloids in saturated consolidated porous media: experimental study," *Colloids Surf. Physicochem. Eng. Asp.*, vol. 352, no. 1, pp. 5–11, 2009.

[12] M. W. Hahn, D. Abadzic, and C. R. O'Melia, "Aquasols: On the role of secondary minima," *Environ. Sci. Technol.*, vol. 38, no. 22, pp. 5915–5924, 2004.

[13] M. W. Hahn, D. Abadzic, and C. R. O'Melia, "Aquasols: On the role of secondary minima," *Environ. Sci. Technol.*, vol. 38, no. 22, pp. 5915–5924, 2004.

[14] X. Li, C.-L. Lin, J. D. Miller, and W. P. Johnson, "Role of grain-to-grain contacts on profiles of retained colloids in porous media in the presence of an energy barrier to deposition," *Environ. Sci. Technol.*, vol. 40, no. 12, pp. 3769–3774, 2006.

[15] J. A. Bergendahl and D. Grasso, "Mechanistic basis for particle detachment from granular media," *Environ. Sci. Technol.*, vol. 37, no. 10, pp. 2317–2322, 2003.

[16] M. M. Sharma, H. Chamoun, D. S. R. Sarma, and R. S. Schechter, "Factors controlling the hydrodynamic detachment of particles from surfaces," *J. Colloid Interface Sci.*, vol. 149, no. 1, pp. 121–134, 1992.

[17] G. K. Darbha, T. Schäfer, F. Heberling, A. Lüttge, and C. Fischer, "Retention of latex colloids on calcite as a function of surface roughness and topography," *Langmuir*, vol. 26, no. 7, pp. 4743–4752, 2010.

[18] D. Gharbi, H. Bertin, and A. Omari, "Use of a gamma ray attenuation technique to study colloid deposition in porous media," *Exp. Fluids*, vol. 37, no. 5, pp. 665–672, 2004.

[19] P. R. Johnson and M. Elimelech, "Dynamics of colloid deposition in porous media: Blocking based on random sequential adsorption," *Langmuir*, vol. 11, no. 3, pp. 801–812, 1995.

[20] C.-H. Ko and M. Elimelech, "The shadow effect in colloid transport and deposition dynamics in granular porous media: measurements and mechanisms," *Environ. Sci. Technol.*, vol. 34, no. 17, pp. 3681–3689, 2000.

[21] G. Chauveteau, L. Nabzar, J. Coste, and others, "Physics and modeling of permeability damage induced by particle deposition," in *SPE Formation Damage Control Conference*, 1998.

[22] J. Happel, "Viscous flow in multiparticle systems: slow motion of fluids relative to beds of spherical particles," *AIChE J.*, vol. 4, no. 2, pp. 197–201, 1958.

[23] M. A. Hubbe, "Detachment of colloidal hydrous oxide spheres from flat solids exposed to flow 2. Mechanism of release," *Colloids Surf.*, vol. 16, no. 3, pp. 249–270, 1985.

[24] N. Sefrioui, A. Ahmadi, A. Omari, and H. Bertin, "Numerical simulation of retention and release of colloids in porous media at the pore scale," *Colloids Surf. Physicochem. Eng. Asp.*, vol. 427, pp. 33–40, 2013.

[25]   S. Vincent, J. C. B. De Motta, A. Sarthou, J.-L. Estivalezes, O. Simonin, and E. Climent, "A Lagrangian VOF tensorial penalty method for the DNS of resolved particle-laden flows," *J. Comput. Phys.*, vol. 256, pp. 582–614, 2014.

[26]   E. M. Hoek and G. K. Agarwal, "Extended DLVO interactions between spherical particles and rough surfaces," *J. Colloid Interface Sci.*, vol. 298, no. 1, pp. 50–58, 2006.

[27]   S. Bhattacharjee and M. Elimelech, "Surface element integration: a novel technique for evaluation of DLVO interaction between a particle and a flat plate," *J. Colloid Interface Sci.*, vol. 193, no. 2, pp. 273–285, 1997.

[28]   E. Martines, L. Csaderova, H. Morgan, A. Curtis, and M. Riehle, "DLVO interaction energy between a sphere and a nano-patterned plate," *Colloids Surf. Physicochem. Eng. Asp.*, vol. 318, no. 1, pp. 45–52, 2008.

[29]   J. B. de Motta, W.-P. Breugem, B. Gazanion, J.-L. Estivalezes, S. Vincent, and E. Climent, "Numerical modelling of finite-size particle collisions in a viscous fluid," *Phys. Fluids 1994-Present*, vol. 25, no. 8, p. 083302, 2013.

[30]   J.-P. Caltagirone and S. Vincent, "Sur une méthode de pénalisation tensorielle pour la résolution des équations de Navier–Stokes," *Comptes Rendus Académie Sci.-Ser. IIB-Mech.*, vol. 329, no. 8, pp. 607–613, 2001.

[31]   W. Johnson, X. Li, and G. Yal, "Colloid retention in porous media: Mechanistic confirmation of wedging and retention in zones of flow stagnation," *Environ. Sci. Technol.*, vol. 41, no. 4, pp. 1279–1287, 2007.

[32]   X. Li, C.-L. Lin, J. D. Miller, and W. P. Johnson, "Role of grain-to-grain contacts on profiles of retained colloids in porous media in the presence of an energy barrier to deposition," *Environ. Sci. Technol.*, vol. 40, no. 12, pp. 3769–3774, 2006.

[33]   X. Li, P. Zhang, C. Lin, and W. P. Johnson, "Role of hydrodynamic drag on microsphere deposition and re-entrainment in porous media under unfavorable conditions," *Environ. Sci. Technol.*, vol. 39, no. 11, pp. 4012–4020, 2005.